ELSEVIER

Journal of Nuclear Materials 305 (2002) 153–158

journal of nuclear materials

www.elsevier.com/locate/jnucmat

Microstructural evolution of nickel-doped 9Cr steels irradiated in HFIR

N. Hashimoto *, R.L. Klueh

Metals and Ceramics Division, Oak Ridge National Laboratory, P.O. Box 2008, Building 4500S MS 6136, Oak Ridge, TN 37831-6136, USA

Received 14 February 2002; accepted 17 July 2002

Abstract

The microstructures of reduced-activation ferritic/martensitic steels, 9Cr–1MoVNb, 9Cr–1MoVNb–2Ni, 9Cr–2WVTa and 9Cr–2WVTa doped with 2% Ni, irradiated at 400 °C up to 12 dpa in the high flux isotope reactor, were investigated by transmission electron microscopy. The cavity number density of Ni-doped steels was higher than that of Ni-undoped steels due to the higher concentration of helium. There was no difference of cavity number density between the steels tempered at 700 and 750 °C, but the mean size of the cavities in the steels tempered at 750 °C was larger than that tempered at 700 °C. There was a tendency for the number density of loops in Ni-doped steels to be higher than in Ni-undoped steels. In addition, the mean size of loops in the steels tempered at 750 °C was larger than for those tempered at 700 °C, while there was not much difference of number density between them. In the steels doped with Ni, irradiation-produced precipitates, identified as $M_6C(\eta)$-type carbide and M_2X phase, were found in the 9Cr–2VWTa–2Ni steel and 9Cr–1MoVNb–2Ni, respectively. Irradiation of Ni-doped steels showed the effect of helium on cavity nucleation, however, the effect of helium on dislocation structure and precipitation was not made clear.

1. Introduction

Ferritic/martensitic steels are attractive candidate structural first wall materials for fusion energy systems [1]. The high-energy neutrons produced by the D–T fusion reaction induce displacement damage and generate gas atoms (H and He) in the materials from (n, p) and (n, α) reactions. It is considered that the simultaneous production of helium atoms from (n, α) reactions could strongly influence the nucleation of cavities. Therefore, to clarify the effect of helium atoms on the microstructural development and mechanical property change in martensitic steels under fast neutron irradiation, 9Cr–1MoVNb, 9Cr–1MoVNb doped with 2%Ni (9Cr–1MoVNb–2Ni), 9Cr–2WVTa and 9Cr–2WVTa doped with 2%Ni (9Cr–2WVTa–2Ni) were irradiated with neutrons in the high flux isotope reactor (HFIR). In this experiment, specimens tempered at different temperature were prepared in order to investigate the effect of tempering on microstructural evolution during irradiation. Irradiation of Ni-doped steels in a mixed spectrum reactor like the HFIR results in the following transmutation reaction with the thermal neutrons: $^{58}Ni(n, \gamma)^{59}Ni(n, \alpha)^{56}Fe$, thus providing the possibility of studying the effects of the simultaneous production of displacement damage and helium production.

2. Experimental procedure

The 9Cr–1MoVNb and 9Cr–1MoVNb–2Ni were normalized by austenitizing 0.5 h at 1050 °C followed by rapid cool in blowing helium, and tempered 1 h at 700 °C.

* Corresponding author. Tel.: +1-865 576 2714; fax: +1-865 241 3650.
E-mail address: hashimoton@ornl.gov (N. Hashimoto).

0022-3115/02/$ - see front matter © 2002 Elsevier Science B.V. All rights reserved.
PII: S0022-3115(02)01026-7

And the 9Cr–2WVTa and the 9Cr–2WVTa–2Ni, normalized 0.5 h at 1050 °C and tempered 1 h at 700 °C (-A) or 750 °C (-B), were also prepared for this experiment. The compositions are given in Table 1. Standard 3-mm diameter transmission electron microscopy (TEM) disks were punched from 0.25-mm thick sheet stock. Irradiation was at 400 °C in the HFIR-CTR-63 target capsule in the HFIR to a neutron fluence of about 1.68×10^{26} n/m^2 ($E > 0.1$ MeV) [2], resulting in a displacement dose of about 12 dpa. The details of the design, construction and installation of HFIR-CTR-62/63 have been reported [3]. The irradiation conditions and the calculated helium concentrations in the steels are given in Table 2. TEM specimens were thinned using an automatic Tenupol electropolishing unit located in a shielded glove box. TEM disks were examined using a JEM-2000FX (LaB_6) transmission electron microscope. The foil thickness was measured using thickness fringes in order to evaluate quantitative defect density values.

Table 1
Chemical compositions of the specimens (wt%)

	9Cr–1MoVNb	9Cr–1MoVNb–2Ni	9Cr–2WVTa	9Cr–2WVTa–2Ni
Cr	8.64	8.54	8.71	8.55
Ni	0.10	2.18	0.02	2.01
Mo	0.97	0.97	2.17	2.15
Nb	0.064	0.068	0.23	0.23
V	0.21	0.22	0.06	0.06
Mn	0.35	0.35	0.39	0.38
W	0.01	<0.01	0.021	0.021
Ta	–	–	<0.01	<0.01
Al	0.013	0.015	<0.01	<0.01
Cu	0.03	0.04	<0.001	<0.001
Ti	0.002	0.002	<0.01	<0.01
C	0.091	0.070	0.098	0.098
P	0.008	0.008	0.014	0.014
S	0.004	0.004	0.003	0.003
Si	0.07	0.08	0.19	0.19
B	<0.001	<0.001	<0.001	<0.001
N	0.050	0.054	0.016	0.016
Fe	Balance	Balance	Balance	Balance

Table 2
Irradiation conditions and helium concentration

	dpa	appm He	He/dpa
9Cr–1MoVNb	12.1	30	2.5
9Cr–1MoVNb–2Ni	12.3	161	13.1
9Cr–2WVTa	12.0	25	2.1
9Cr–2WVTa–2Ni	12.3	150	12.2

3. Results

3.1. Dislocations and dislocation loops

Fig. 1 shows the dislocation segments and loops in the steels after irradiation at 400 ° C to 12 dpa using the diffraction conditions $g = 110$ $(g, 4g)$. During irradiation of Fe–Cr binary alloys, dislocation evolution in an initially almost dislocation-free condition proceeds by the formation of interstitial-type dislocation loops with an $a_0\langle 1\,0\,0\rangle$ and/or $(a_0/2)\langle 1\,1\,1\rangle$ Burgers vector [4,5]. Similar loops form in more complicated steels [6,7], such as those used in this experiment. Table 3 summarizes the quantitative results of the dislocation loops observed. The number density and the mean diameter of $a_0\langle 1\,0\,0\rangle$ type loops are higher and smaller than that of

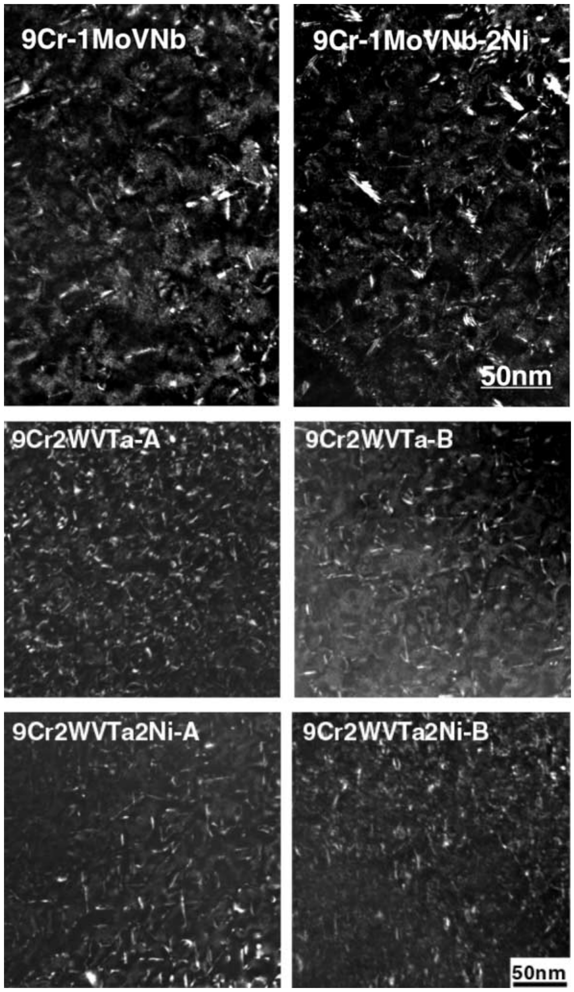

Fig. 1. Dislocation segments and loops in 9Cr–1MoVNb and 9Cr–1MoVNb–2Ni, 9Cr–2WVTa-A, 9Cr–2WVTa-B, 9Cr–2WVTa–2Ni-A and 9Cr–2WVTa–2Ni-B after irradiation at 400 °C to 12 dpa using the diffraction conditions: $g = 110$ $(g, 4g)$.

Table 3
Summary of dislocation structure after irradiation

Steel	$a_0\langle 100\rangle$ type loops		$(a_0/2)\langle 111\rangle$ type loops	
	Number density (m^{-3})	Mean diameter (nm)	Number density (m^{-3})	Mean diameter (nm)
9Cr–1MoVNb	5×10^{21}	21	4×10^{21}	25
9Cr–1MoVNb–2Ni	7×10^{21}	20	6×10^{21}	24
9Cr–2WVTa-A	1×10^{22}	18	5×10^{21}	28
9Cr–2WVTa–2Ni-A	1×10^{22}	17	6×10^{21}	16
9Cr–2WVTa-B	1×10^{22}	23	4×10^{21}	30
9Cr–2WVTa–2Ni-B	1×10^{22}	23	6×10^{21}	28

$(a_0/2)\langle 111\rangle$ type loops for all the steels. In addition, there is a tendency for a higher number density of $(a_0/2)\langle 111\rangle$ type loops in Ni-doped steels compared to undoped steels. With respect to the two different tempering temperatures, the mean size of the loops in the steels tempered at 750 °C was larger than for those tempered at 700 °C, while there was little difference in the number density between them. Before irradiation, the dislocation density of specimens tempered at 700 °C were higher than for those tempered at 750 °C, and higher dislocation density tends to cause a smaller size of loops during irradiation. This suggests that the growth of irradiation-induced loops is controlled by heat treatment before irradiation.

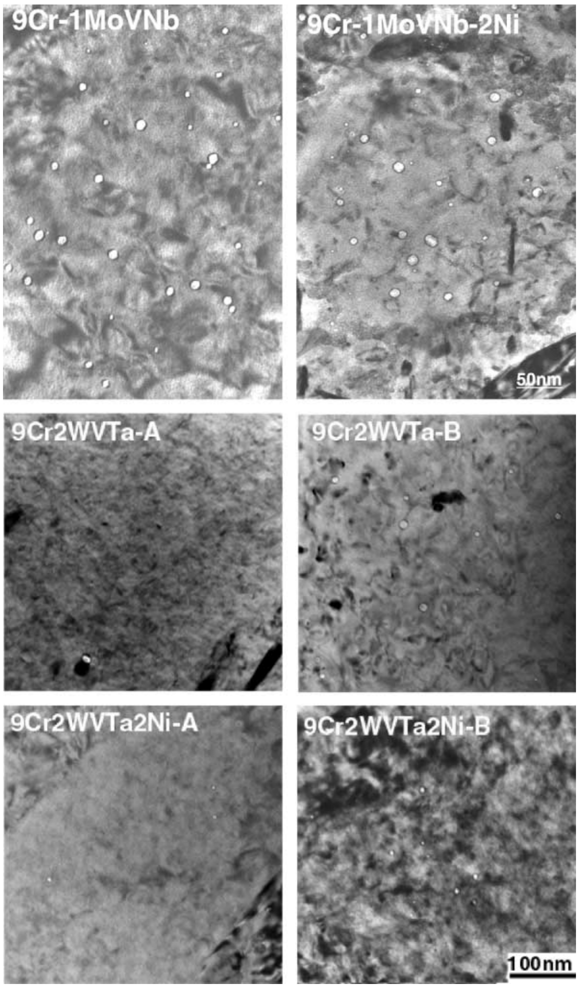

Fig. 2. Cavities in 9Cr–1MoVNb and 9Cr–1MoVNb–2Ni, 9Cr–2WVTa-A, 9Cr–2WVTa-B, 9Cr–2WVTa–2Ni-A and 9Cr–2WVTa–2Ni-B after irradiation at 400 °C to 12 dpa.

3.2. Cavities

Fig. 2 shows cavities of the specimens irradiated at 400 °C to 12 dpa. Distribution of cavities is homogeneous in the matrices, and no cavities were observed on grain boundaries. Neutron irradiation induced tiny cavities (5 nm) with the number densities of 9×10^{21} m^{-3} in 9Cr–1MoVNb–2Ni. In 9Cr–1MoVNb, somewhat larger cavities (9 nm) with the number densities of 3×10^{21} m^{-3} were observed. Swelling of 9Cr–1MoVNb and 9Cr–1MoVNb–2Ni were 0.17% and 0.15%, respectively. In 9Cr–2WVTa-A and -B, somewhat larger cavities were observed even though this steel contained very little helium compared with the Ni-doped steels. Swelling of these steels was estimated to be <0.05%. Table 4 summarizes the quantitative results of the observations on the cavities.

Table 4
Summary of cavities formed during irradiation

Steel	Mean size (nm)	Number density (m^{-3})	Swelling (%)
9Cr–1MoVNb	9	3×10^{21}	0.17
9Cr–1MoVNb–2Ni	5	9×10^{21}	0.15
9Cr–2WVTa-A	3	1×10^{21}	<0.002
9Cr–2WVTa–2Ni-A	3	3×10^{21}	<0.006
9Cr–2WVTa-B	9	1×10^{21}	0.05
9Cr–2WVTa–2Ni-B	4	3×10^{21}	0.02

3.3. Precipitates

Before irradiation, the precipitates in all the steels used in this study include $M_{23}C_6$ on grain and/or lath boundaries, with the number density and the mean diameter of $< 1 \times 10^{20}$ m^{-3} and about 100 nm, respectively. There was no difference in the temper-induced $M_{23}C_6$ before and after irradiation in terms of size and distribution, but neutron irradiation did produce additional precipitates in the matrices of the Ni-doped steels. The spacing of moiré fringes was used to identify the irradiation-produced precipitates, which were identified as M_2X phase in the 9Cr–1MoVNb–2Ni and $M_6C(\eta)$-type carbide in the 9Cr–2VWTa–2Ni. Fig. 3 shows the irradiation-induced precipitates in the 9Cr–1MoVNb–2Ni and the 9Cr–2VWTa–2Ni after irradiation at 400 °C to 12 dpa. Precipitation of a Cr- and Ni-rich $M_6C(\eta)$ has been observed in a number of 8–12Cr steels that contain >0.3 wt% Ni during fast breeder reactor and HFIR irradiation at about 400 °C [8–11]. Table 5 summarizes the quantitative results of precipitates.

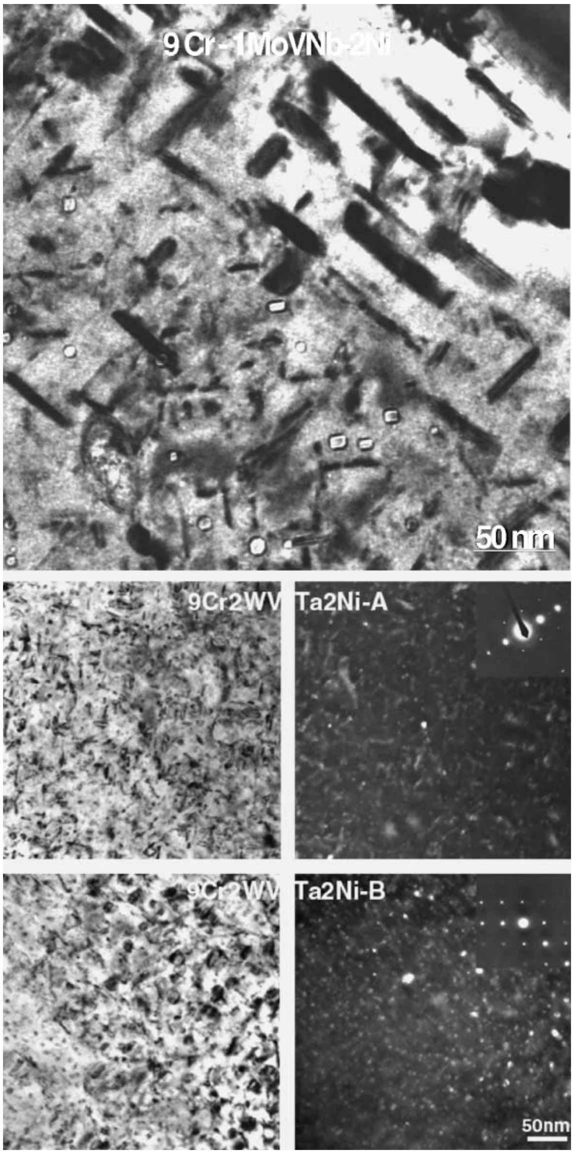

Fig. 3. Irradiation-induced precipitates in 9Cr–1MoVNb–2Ni, 9Cr–2VWTa–2Ni-A and 9Cr–2VWTa–2Ni-B after irradiation at 400 °C to 12 dpa.

4. Discussion

The results from the TEM observations, some of which appear to differ from previous studies, provide information on the effect of composition (W, Mo, N, Ni, etc.) on the irradiation behavior of the steels. Prior to irradiation, the microstructures of all the steels had similar dislocation line densities ($2–7 \times 10^{14}$ m^{-2}) and precipitates, which were mainly $M_{23}C_6$ ($\approx$100 nm in diameter and a number density of $<10^{20}$ m^{-3}) with a few MC precipitates, mainly on dislocations.

Irradiation of Ni-containing steels in HFIR results in the formation of helium from an (n, α) reaction with thermal neutrons. The amount of helium in the Ni-doped steels would be approximately 5–6 times higher than that in the undoped steels (Table 2). Results from the present work indicate that the Ni-doped steels have a tendency to include higher density of cavities and partially higher swelling than the undoped steels. Although the amount of swelling was small, there was an effect of helium, especially for the 9Cr–2WVTa and 9Cr–2WVTa–2Ni steels, with the latter steel swelling three times as much as the former (0.006% vs. 0.002%). Three times as many cavities were observed for the 9Cr–2WVTa–2Ni than for 9Cr–2WVTa, which was similar to the difference in cavity density observed for the 9Cr–1MoVNb–2Ni and 9Cr–1MoVNb steels, indicating the effect of helium on cavity nucleation. Irradiation of Ni-containing steels also slightly affected the formation of dislocation loops; however, the difference between Ni-doped and undoped steels was small. From this experiment, the effect of helium on dislocation structure was not made clear.

Results from the present work also indicate that the 9Cr–1MoVNb steels have a tendency to swell more than some other ferritic/martensitic steels [12–15]. The results also indicate that composition of elements other than the 9%Cr has an effect on the swelling. Although neither steel showed large amounts of swelling, the swelling in the 9Cr–1MoVNb steel was more than twice that in the 9Cr–2WVTa steel. This agrees with previous work [13], where the 9Cr–1MoVNb, 9Cr–2WVTa and 9Cr–2WV (the same as the 9Cr–2WVTa, but without the 0.01% tantalum) steels were irradiated in FFTF at $\approx$420 °C to

Table 5
Summary of precipitates in the steels after irradiation at 400 °C

Steel	$M_{23}C_6$		M_2X		$M_6C(\eta)$	
	Mean size (nm)	Number density (m^{-3})	Mean size (nm)	Number density (m^{-3})	Mean size (nm)	Number density (m^{-3})
9Cr–1MoVNb	95	$<1 \times 10^{20}$	–	–	–	–
9Cr–1MoVNb–2Ni	98	$<1 \times 10^{20}$	54	5×10^{20}	–	–
9Cr–2VWTa-A	95	$<1 \times 10^{20}$	–	–	–	–
9Cr–2VWTa–2Ni-A	92	$<1 \times 10^{20}$	–	–	7	2×10^{21}
9Cr–2VWTa-B	102	$<1 \times 10^{20}$	–	–	–	–
9Cr–2VWTa–2Ni-B	98	$<1 \times 10^{20}$	–	–	6	2×10^{21}

35 dpa. Swelling for the three steels was estimated as 0.85%, 0.33% and 0.2%, respectively, again demonstrating the effect of composition, with the standard 9Cr–1MoVNb steel showing the highest swelling. However, it must be noted that the 12Cr–1MoVW steel irradiated in that experiment showed only 0.007% swelling, giving further credence to the conclusion that 9Cr steels have a tendency to swell more that 12Cr steels [12–16]. One reason for the lower swelling resistance of the 9Cr–1MoVNb that the other 9Cr steels might be the nitrogen added to this steel. The 9Cr–1MoVNb with 0.054% N contains twice as much nitrogen as the 12Cr–1MoVW (0.027% N). However, the 9Cr–2WVTa (0.029% N) and the 9Cr–2WV (0.022% N) contain amounts similar to the 12Cr–1MoVW steel, indicating that nitrogen is not the sole determinant for the difference between the 9Cr–1MoVNb and the other 9Cr steels and the 12Cr steel. Previous work for neutron-irradiated austenitic stainless steels reported an effect of nitrogen on swelling [17], in which the presence of 0.02% nitrogen resulted in large swelling. Some ion irradiation experiments indicated that residual oxygen chemisorption led to a lower cavity surface energy and, therefore, affected the swelling [18,19]. However, nitrogen would not be expected to have such a strong chemical effect.

The difference in the precipitates after irradiation between 9Cr–1MoVNb–2Ni and 9Cr–2WVTa–2Ni steels is of interest. Whereas the 9Cr–2WVTa–2Ni contained a high-number density (2×10^{21} m^{-3}) of small (7 nm) nickel-rich M_6C particles, the 9Cr–1MoVNb–2Ni steel contained a smaller number density (5×10^{20} m^{-3}) of larger (54 nm) M_2X particles. A previous investigation found nickel-rich M_6C precipitates in 9Cr–1MoV-Nb–2Ni and 9Cr–1MoVW–2Ni [12,13] after irradiation in both FFTF and HFIR. Nickel-rich precipitates were also found in ternary Fe–12Cr–1.5Ni alloys irradiated at 300 and 400 °C in HFIR [20]. The M_6C precipitates in the 9Cr–1MoVNb–2Ni were found after irradiation to 47 dpa at 407 °C in FFTF and 37 dpa at 400 °C in HFIR [12,13]. Traces of M_2X were found in the 9Cr–1MoVNb and the 9Cr–1MoVNb–2Ni steels that were irradiated in FFTF but not in those irradiated in HFIR [12,13]. The M_2X is a Cr-rich precipitate with the X generally high in nitrogen, which would be in accord with the 9Cr–1MoVNb steel containing a higher nitrogen concentration than the other steels. The reason for not finding the high density of M_6C in the 9Cr–1MoVNb–2Ni in the present experiment is unknown; it may mean that the M_2X forms first (low dpa) followed by the formation of the M_6C. This is consistent with the lower dose of the present experiment irradiation (12 dpa), compared to about 40 dpa in the previous experiments [12,13]. This Ni-doping experiment showed the difference in the precipitates in the steels, but the helium effect on precipitation is uncertain.

In addition to the TEM specimens of the nickel-doped steels that were used to determine the effect of helium on swelling and microstructure, discussed in this paper, the irradiation capsule also contained tensile and Charpy impact specimens of 9Cr–1MoVNb, 9Cr–1MoVNb–2Ni, 9Cr–2WVTa and 9Cr–2WVTa–2Ni steels. Results on the effect of irradiation on the tensile and Charpy properties of the irradiated 9Cr–2WVTa and 9Cr–2WVTa–2Ni steels have been published [21]. The implication of the microstructural observations discussed here on the mechanical properties of those steels will be deferred to a future paper that will present the mechanical properties of the irradiated 9Cr–1MoVNb and 9Cr–1MoVNb–2Ni steels.

5. Summary

To determine the effect of helium on the microstructure of 9Cr–1MoVNb and 9Cr–2WVTa steels, alloys with these compositions along with similar containing 2% Ni (9Cr–1MoVNb–2Ni and 9Cr–2WVTa–2Ni) were irradiated in HFIR. Irradiation of Ni-containing steels in HFIR results in the formation of helium from an (n, α) reaction with thermal neutrons.

Although the amount of swelling was small, there was an effect of helium, especially for the 9Cr–2WVTa and

9Cr–2WVTa–2Ni steels, with the latter steel swelling three times as much as the former (0.006% vs. 0.002%). Swelling for both the 9Cr–2WVTa and 9Cr–2WVTa–2Ni steels was estimated at <0.05%. Three times as many cavities were observed for the 9Cr–2WVTa–2Ni than for 9Cr–2WVTa, which was similar to the difference in cavity density observed for the 9Cr–1MoVNb–2Ni and 9Cr–1MoVNb steels, indicating the effect of helium on cavity nucleation. However, the effect of helium on dislocation structure and precipitation is still uncertain.

Before irradiation, all four steels contained similar precipitates: mainly $M_{23}C_6$ with a few MC precipitates. After irradiation, no change in precipitates was observed for the steels without nickel. However, irradiation-induced precipitates were observed in the nickel-containing steels, with the 9Cr–1MoVNb–2Ni containing a low-number density of M_6C and the 9Cr–1MoVNb–2Ni containing M_2X. The presence of M_2X instead of M_6C may have been due to the nitrogen in the 9Cr–1MoVNb–2Ni along with a lower fluence of the present experiment compared to previous higher-dose irradiations where M_6C was observed.

Acknowledgements

The authors would like to thank Messrs J.W. Jones and J.J. Duff for technical support. Particular thanks go to Mr L.T. Gibson for the preparation of TEM specimens for microstructural examination. This research was supported in part by an appointment to the Oak Ridge National Laboratory Postdoctoral Research Associates Program administered jointly by the Oak Ridge Institute for Science and Education and Oak Ridge National Laboratory.

References

[1] R.L. Klueh, K. Ehrlich, F. Abe, J. Nucl. Mater. 191–194 (1992) 116.
[2] L.R. Greenwood, C.A. Baldwin, Neutron dosimetry and damage calculations for the HFIR-CTR-62 and 63 irradiations, Fusion Reactor Materials Semiannual Report for Period Ending June 30, 1999, DOE/ER-0313/26, 1999, p. 199.
[3] K.E. Lenox, R.L. Klueh, R.L. Senn, Continuing irradiation of ferritic steels: experiments HFIR-CTR-62 and -63, Fusion Reactor Materials Semiannual Report for Period Ending March 31, 1995, DOE/ER-0313/18, 1995, p. 7.
[4] N. Yoshida et al., J. Nucl. Mater. 155–157 (1988) 1232.
[5] D.S. Gelles, in: N.H. Packan, R.E. Stoller, A.S. Kumar (Eds.), Effects of Irradiation on Materials – 14th International Symposium, ASTM STP 1046, vol. 1, American Society for Testing and Materials, Philadelphia, PA, 1989, p. 73.
[6] D.S. Gelles, J. Nucl. Mater. 233–237 (1996) 293.
[7] N. Hashimoto, R.L. Klueh, Microstructural evolution of 9Cr–2WVTa steels in HFIR-CTR-62/63 experiment, Fusion Reactor Materials Semiannual Report for Period Ending June 30, 2000, DOE/ER-0313/28, 2000, p. 147.
[8] E.A. Little, L.P. Stoter, in: Effects of Radiation on Materials – 11th Conference, ASTM STP-782, American Society for Testing and Materials, Philadelphia, PA, 1982, p. 207.
[9] P.J. Maziasz, R.L. Klueh, J.M. Vitek, J. Nucl. Mater. 141–143 (1986) 929.
[10] P.J. Maziasz, R.L. Klueh, in: Effects of Radiation on Materials – 14th Conference, ASTM STP-1046, American Society for Testing and Materials, Philadelphia, PA, 1989, p. 35.
[11] P.J. Maziasz, J. Nucl. Mater. 169 (1989) 95.
[12] P.J. Maziasz, R.L. Klueh, J.M. Vitek, J. Nucl. Mater. 141–143 (1986) 929.
[13] P.J. Maziasz, R.L. Klueh, in: N.H. Packan, R.E. Stoller, A.S. Kumear (Eds.), Effects of Irradiation on Materials – 14th International Symposium, ASTM STP 1046, vol. 1, American Society for Testing and Materials, Philadelphia, PA, 1989, p. 35.
[14] D.S. Gelles, J. Nucl. Mater. 233–237 (1996) 293.
[15] J.J. Kai, R.L. Klueh, J. Nucl. Mater. 230 (1996) 116.
[16] D.S. Gelles, J. Nucl. Mater. 212–215 (1994) 714.
[17] N. Hashimoto, E. Wakai, J.P. Robertson, T. Sawai, A. Hishinuma, J. Nucl. Mater. 280 (2000) 186.
[18] E.H. Lee, L.K. Mansur, Philos. Mag. A 61 (1990) 751.
[19] S.J. Zinkle, E.H. Lee, Met. Trans. A 21 (1990) 1037.
[20] D.S. Gelles, in: Effects of Irradiation on Materials – 18th International Symposium, ASTM STP 1325, American Society for Testing and Materials, West Conshohocken, PA, 1999, p. 899.
[21] R.L. Klueh, M.A. Sokolov, K. Shiba, J.P. Robertson, J. Nucl. Mater. 283–287 (2000) 478.